Phase Diagram and Impedance Spectroscopy Study of the $La_{0.5+x-y}Bi_yLi_{0.5-3x}TiO_3$ System

M.-L. Martínez-Sarrión,*[a] L. Mestres,[a] M. Herráiz,[a] O. Maqueda,[a] A. Bakkali,[a] and N. Fernández[b]

Keywords: Phase diagrams / Perovskite phases / Conducting materials / Lanthanides

The phase diagram of the system $Li_2O/La_2O_3/TiO_2/Bi_2O_3$ has been studied. Using powder X-ray diffraction, five distinct areas have been found in the triangle $Bi_{0.5}Li_{0.5}TiO_3/La_{2/3}TiO_3/La_{0.5}Li_{0.5}TiO_3$. A region of perovskite-like solid solutions was obtained when the bismuth content in the general formula $La_{0.5+x-y}Bi_yLi_{0.5-3x}TiO_3$ was less than y = 0.10. Two two-phase regions, one of them consisting of a perovskite-like phase and $La_2Ti_2O_7$, and the other a perovskite-like phase and Li_2TiO_3, were obtained. One four-phase region, consisting of a perovskite-like phase, Li_2TiO_3, $Bi_4Ti_3O_{12}$ and $La_4Ti_3O_{12}$, was also obtained. The fifth area corresponds to the melting of the initial mixtures. The microstructures of these phases were studied by SEM/EDS. The compounds of general formula $La_{0.5+x-y}Bi_yLi_{0.5-3x}TiO_3$ are ionic conductors. Their ionic conductivity increases when the amount of lithium rises up to x = 0.075, and decreases when the amount of bismuth increases.

Introduction

With the development of advanced materials in which the fine-tuning of composition is often required in order to optimize properties, phase diagrams take on the increasingly important role of representing phase stoichiometries. The phase diagram contains qualitative structural information as well as quantitative compositional information, and together they provide a powerful basis for understanding and optimising relationships between stoichiometry, structure and properties.

Research into solid ionic conductors and lithium cathodes is important for the development of solid-state lithium batteries. Some time ago, fast ion conductors with the general formula $RE_{0.5+x}Li_{0.5-3x}TiO_3$, where RE = La, Pr, Nd, and Sm, were reported.[1−3] The maximum bulk conductivity was found in the lanthanum system, with a value of 1.1×10^{-3} S·cm^{-1} for $x = 0.07$, although the total conductivity (bulk and grain boundary conductivity), was less than 10^{-6} S·cm^{-1}. More recently, the phase diagram, crystal chemistry and ion conductivity of the systems $RE_{0.5+x}Li_{0.5-3x}TiO_3$, (RE = La, Pr, Nd),[4−7] which show a similar total conductivity, have been reported.

In recent years, the phase diagrams, crystal chemistry and conductivity study of $Pr_{0.5+x+y}Li_{0.5-3x}Ti_{1-3y}Cr_{3y}O_3$,[8] $La_{0.5+x+y}Li_{0.5-3x}Ti_{1-3y}Mn_{3y}O_3$,[9] and $La_{0.5+x+y}Li_{0.5-3x}Ti_{1-3y}Cr_{3y}O_3$,[10] have been reported.

Systems containing Bi_2O_3 are now becoming increasingly important in the technology of new materials used by the electronics industry. Levin and Roth[11] studied 33 systems with bismuth oxide as one of the components. The content of the other components was never higher than 10−15 mol %. The binary systems Bi_2O_3/Li_2O, Bi_2O_3/TiO_2, and Bi_2O_3/La_2O_3 were described.

Bi_2O_3 has two stable crystalline forms: a low-temperature monoclinic form and a high-temperature cubic form, and the conversion of one form into the other takes place at 730 °C. Many systems typically form solid solutions based on bismuth oxide.

Doped $Bi_4V_2O_{11}$ materials are currently under intensive study in several laboratories because of their attractive electrical properties. They are, however, complex materials both structurally and compositionally as the $Bi_4V_2O_{11}$ phase has a variable Bi:V ratio.[12−14]

The aim of the present work was to investigate the synthesis and the stoichiometry range of the new compounds of general formula $La_{0.5+x-y}Bi_yLi_{0.5-3x}TiO_3$ and to establish the phase diagram at room temperature of the system $La_{2/3}TiO_3$-$Bi_{0.5}Li_{0.5}TiO_3$-$La_{0.5}Li_{0.5}O_3$. The substitution of lanthanum by bismuth in $La_{0.5+x}Li_{0.5-3x}TiO_3$ may affect the ionic conductivity of these compounds, therefore changes in the electric behaviour of the

[a] Departament de Química Inorgànica, Universitat de Barcelona
Martí i Franquès 1−11, 08028 Barcelona, Spain
Fax: (internat.) + 34-93/490-7725
E-mail: marialuisa.martinez@qi.ub.es
[b] Departamento de Química Inorgánica, Universidad de La Habana,
La Habana, Cuba

Table 1. Sample composition

Starting composition				Experimental composition				Phase
La	Bi	Li	Ti	La	Bi	Li	Ti	
0.55	0.00	0.35	1.00	0.59	0.00	0.32	1.00	Perovskite-like phase
0.57	0.00	0.30	1.00	0.60	0.00	0.27	1.00	Perovskite-like phase
0.58	0.00	0.25	1.00	0.63	0.00	0.23	1.00	Perovskite-like phase
0.60	0.00	0.20	1.00	0.64	0.00	0.18	1.00	Perovskite-like phase
0.57	0.010	0.25	1.00	0.60	0.008	0.24	1.00	Perovskite-like phase
0.59	0.010	0.33	1.00	0.55	0.009	0.32	1.00	Perovskite-like phase
0.55	0.02	0.29	1.00	0.55	0.018	0.29	1.00	Perovskite-like phase
0.57	0.040	0.17	1.00	0.59	0.038	0.15	1.00	Perovskite-like phase
0.53	0.040	0.27	1.00	0.53	0.038	0.26	1.00	Perovskite-like phase
0.52	0.040	0.32	1.00	0.55	0.037	0.30	1.00	Perovskite-like phase
0.54	0.046	0.36	1.00	0.51	0.047	0.25	1.00	Perovskite-like phase
0.50	0.055	0.35	1.00	0.46	0.056	0.33	1.00	Perovskite-like phase
0.47	0.060	0.42	1.00	0.50	0.057	0.40	1.00	Perovskite-like phase
0.50	0.10	0.20	1.00	0.47	0.098	0.17	1.00	Perovskite-like phase
0.46	0.070	0.42	1.00	0.48	0.065	0.41	1.00	Perovskite-like phase
0.51	0.075	0.25	1.00	0.52	0.072	0.22	1.00	Perovskite-like phase
0.49	0.075	0.30	1.00	0.47	0.073	0.29	1.00	Perovskite-like phase
0.46	0.075	0.40	1.00	0.48	0.072	0.37	1.00	Perovskite-like phase

$La_{0.5+x-y}Bi_yLi_{0.5-3x}TiO_3$ system are expected, even though bismuth is only a minority element.

Results and Discussion

Phase Diagram

The triangle $Bi_{0.5}Li_{0.5}TiO_3$-$La_{2/3}TiO_3$-$La_{0.5}Li_{0.5}TiO_3$ in the Li_2O-La_2O_3-TiO_2-Bi_2O_3 system was chosen for detailed study since the $La_{2/3}TiO_3$-$La_{0.5}Li_{0.5}TiO_3$ join has been reported previously.[3,15] This triangle was studied by synthesizing compounds of general formula $La_{0.5+x-y}Bi_yLi_{0.5-3x}TiO_3$ by heating, as described in the Exp. Sect. More than 50 different compositions were prepared. The results of X-ray powder diffraction and the results of ICP analysis (Table 1), were used to construct the composition diagram (Figure 1).

Five distinct areas were found on this triangle. A region, (A), resulting from the melting of the initial mixture, a region, (D), of perovskite-like solid solutions (Figure 2a), and three mixed-phase regions (B, C, E). Region C is a mixture of the perovskite-like phase and peaks belonging to $La_2Ti_2O_7$ (identified from PDF 28-517; Figure 2b). Region E is a mixture of the perovskite-like phase and peaks which belong to Li_2TiO_3 (identified from PDF 33-0831; Figure 2c). Region B is a mixture of the perovskite-like phase and peaks identified as Li_2TiO_3 (from PDF 33-0831), $Bi_4Ti_3O_{12}$ (PDF 73-2181) and $La_4Ti_3O_{12}$ (PDF 33-727; Figure 2d) (PDF compiled by JCPDS).

Table 2 shows the X-ray powder diffraction data for $La_{0.51}Bi_{0.047}Li_{0.25}TiO_3$ (region D). This compound has an orthorhombic perovskite-type structure. Table 3 shows the X-ray diffraction data for $La_{0.56}Bi_{0.047}Li_{0.08}TiO_3$ (region C), containing reflections corresponding to an orthorhombic perovskite-type structure, reflections corresponding to $La_2Ti_2O_7$ and some peaks associated with a superstructure.

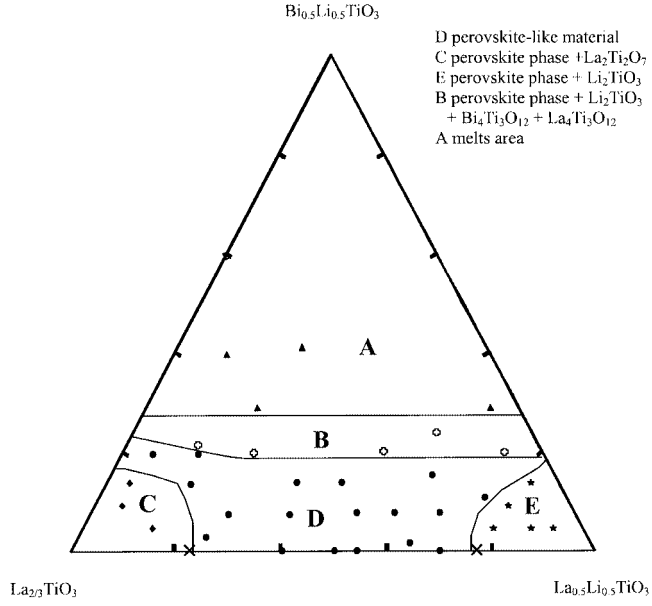

Figure 1. Composition triangle of the system $La_{0.5+x-y}Bi_yLi_{0.5-3x}TiO_3$ at 1250 °C; the samples marked with × are taken from the literature[4]

This superstructure depends on the lithium content and is related to the lanthanum and vacant A-sites that alternates along the *c*-axis. This ordering becomes progressively disordered when the lithium content increases.[16]

Table 4 shows the X-ray powder diffraction data for $La_{0.48}Bi_{0.023}Li_{0.43}TiO_3$ (region E). We observed reflections corresponding to a cubic perovskite-type structure and reflections corresponding to Li_2TiO_3. Finally, Table 5 shows X-ray powder diffraction data for $La_{0.40}Bi_{0.112}Li_{0.47}TiO_3$ (region B). In this region reflections corresponding to a cubic perovskite-type structure, Li_2TiO_3, $Bi_4Ti_3O_{12}$, and $La_4Ti_3O_{12}$ appear.

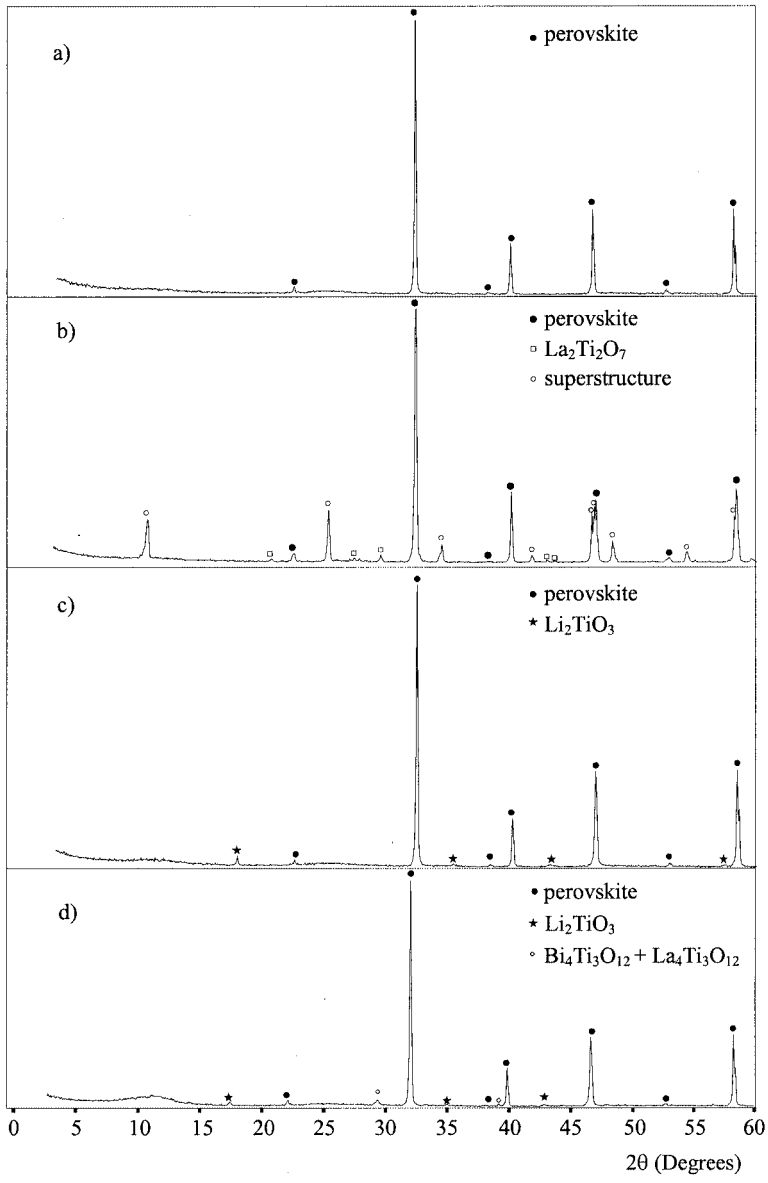

Figure 2. XRD patterns of the five regions on the composition triangle

Table 2. Indexed powder pattern of the single phase $La_{0.51}Bi_{0.047}Li_{0.25}TiO_3$; orthorhombic system: a = 5.487(2) Å, b = 5.472(1) Å, c = 7.739(2) Å, V = 232.38(5) Å^3, Z = 4

hkl	d_{obs}/Å	d_{calc}/Å	I/I_0
002	3.862	3.869	3
200	2.740	2.744	100
112	2.736	2.738	26
103	2.326	2.333	1
202	2.239	2.238	19
022	2.237	2.234	8
004	1.930	1.935	64
222	1.728	1.732	1
114	1.727	1.731	1
204	1.578	1.583	23
132	1.577	1.581	33

Some melting occurs in the compositions in area A. These compositions have a greater content of bismuth (as Bi_2O_3), and as bismuth oxide melts at about 830 °C the formation of the perovskite-like phase is prevented. Some systems containing Bi_2O_3 reported in the literature, such as Bi_2O_3-Li_2O, Bi_2O_3-TiO_2, and Bi_2O_3-La_2O_3, show the *liquidus* area at about 900 °C.[11]

Perovskite-like phases mixed with titanium compounds are obtained in the areas C and E. In the area close to the vertex $La_{2/3}TiO_3$ (area C), $La_2Ti_2O_7$ is segregated along with the perovskite-like phase. On progressing towards the join $La_{2/3}TiO_3$/$La_{0.5}Li_{0.5}TiO_3$ the lithium content increases and Li_2TiO_3 is segregated along with the perovskite-like phase near the $La_{0.5}Li_{0.5}TiO_3$ vertex (area E).

In area B, on increasing the lithium content, the number of species mixed with the perovskite-like phase increases, as

Table 3. Indexed powder pattern of $La_{0.56}Bi_{0.047}Li_{0.08}TiO_3$

d_{obs} [a]	Perovskite		$La_2Ti_2O_7$	
	d/Å	*hkl*	*d*/Å	*hkl*
7.738*		001		
4.192			4.201	−210
3.885	3.862	002		
3.447*		101		
3.208			3.217	400
2.988			2.995	−212
2.752	2.740	200		
2.743	2.736	112		
2.574*		111		
2.336	2.326	103		
2.246	2.239	202		
2.240	2.237	022		
2.148*		103		
2.094			2.101	420
2.069			2.071	−322
1.940	1.930	004		
1.933*		200		
1.878*		201		
1.738	1.728	222		
1.735	1.727	114		
1.686*		211		
1.584	1.578	204		
1.583	1.577	132		

[a] * Superstructure lines.

Table 4. Indexed powder pattern of $La_{0.48}Bi_{0.023}Li_{0.43}TiO_3$

d_{obs}	Perovskite		Li_2TiO_3	
	d/Å	*hkl*	*d*/Å	*hkl*
4.824			4.800	002
3.868	3.862	002		
2.737	2.740	200		
2.733	2.736	112		
2.521			2.502	−131
2.332	2.326	103		
2.235	2.239	202		
2.232	2.237	022		
2.089			2.075	−133
1.933	1.930	004		
1.730	1.728	222		
1.729	1.727	114		
1.579	1.578	204		
1.578	1.577	132		

do their relative amounts. For instance, the maxima of Li_2TiO_3 are not observed and the reflections of the $Bi_4Ti_3O_{12}$ and $La_4Ti_3O_{12}$ components are very weak in the sample of starting composition $La_{0.45}Bi_{0.10}Li_{0.35}TiO_3$. On increasing the lithium content, for example for starting composition $La_{0.41}Bi_{0.10}Li_{0.48}TiO_3$, the perovskite-like phase is mixed with Li_2TiO_3, $Bi_4Ti_3O_{12}$ and $La_4Ti_3O_{12}$, with an increase in the relative intensities.

The cell volume was obtained for two joins on the composition triangle. Along join 1, $La_{0.46+x}Bi_{0.04}Li_{0.5-3x}TiO_3$, the amount of bismuth remained constant, while along join 2, $La_{0.57-y}Bi_yLi_{0.29}TiO_3$, the amount of lithium was constant. The cell volume was measured against the amount of lanthanum along these two joins (Figure 3). For the same

Table 5. Indexed powder pattern of $La_{0.40}Bi_{0.112}Li_{0.47}TiO_3$

d_{obs}	Perovskite		Li_2TiO_3		$Bi_4Ti_3O_{12}$		$La_4Ti_3O_{12}$	
	d/Å	*hkl*	*d*/Å	*hkl*	*d*/Å	*hkl*	*d*/Å	*hkl*
4.811			4.800	002				
4.060			4.050	021				
3.868	3.862	002						
2.969					2.9703	117	2.960	107
2.738	2.740	200						
2.734	2.736	112						
2.640					2.6442	−119		
2.515			2.502	−131				
2.330	2.326	103						
2.270					2.2701	208		
2.235	2.239	202						
2.232	2.237	022						
2.087			2.075	−133				
2.025							2.020	119
1.934	1.930	004						
1.774					1.7714	0214		
1.732	1.728	222						
1.730	1.727	114						
1.581	1.578	204						
1.579	1.577	132						

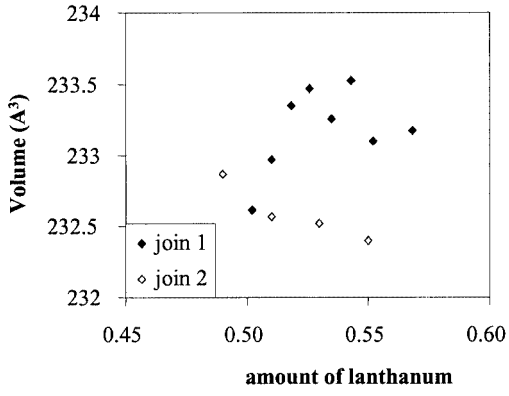

Figure 3. Cell volume vs. La content along the two joins on samples quenched from 1250 °C

amount of bismuth, the cell volume decreases as the lanthanum content decreases, due to the substitution of lanthanum by a smaller cation such as lithium in the 12-coordinate sites. Along join 2, the substitution of lanthanum by bismuth leads to a small increase in the cell volume because of the different ionic radii.

The composition with the highest conductivity in the join $La_{2/3}TiO_3$-$La_{0.5}Li_{0.5}TiO_3$ is $La_{0.57}Li_{0.29}TiO_3$.[1−3] The new conductors should occur in the join $La_{0.57}Li_{0.29}TiO_3$-$Bi_{0.5}Li_{0.5}TiO_3$. The compositions of the new phases containing bismuth should have lanthanum and lithium contents close to $La_{0.57}Li_{0.29}TiO_3$, with low bismuth contents. This is indeed the case, since the only one-phase compositions with the perovskite structure are those with bismuth contents less than 0.10 in the general formula $La_{0.5+x-y}Bi_yLi_{0.5-3x}TiO_3$.

Scanning Electron Microscopy (SEM, EDS)

A selection of ceramic samples from both within and outside the perovskite single-phase region was analysed by

SEM/EDS. Elemental analyses were carried out with a fixed beam of 10 kV and 20 nA over different points of the sample surface.

Scanning electron micrographs were obtained for samples from each of the four regions observed in the composition triangle, and in all the phases we checked the presence of the different elements by SEM and EDS.

Figure 4a shows the back-scattered electron image (BEI) of the sample $La_{0.51}Bi_{0.047}Li_{0.25}TiO_3$. In this case, homogeneous crystals were observed, which agrees with the XRD pattern shown in Figure 2a. The EDS spectrum of this zone (Figure 5a) shows the presence of lanthanum, bismuth and titanium in a perovskite-like phase for this composition obtained when different crystals of the sample are analysed. Figure 4b shows the BEI of the sample $La_{0.56}Bi_{0.047}Li_{0.08}TiO_3$. In this case we observed similar crystals to Figure 4a (area 1 in the picture) and new gray crystals (area 2 in the picture).

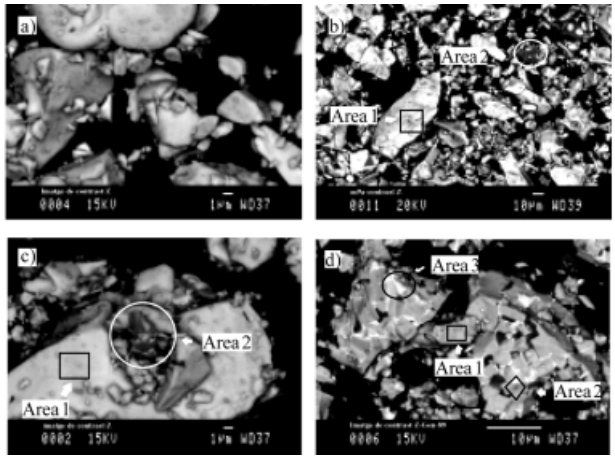

Figure 4. Scanning electron micrographs of: a) perovskite-like single-phase solid solution region; b) perovskite-like phase + $La_2Ti_2O_7$; c) perovskite-like phase + Li_2TiO_3 region; d) perovskite-like phase + Li_2TiO_3, + $Bi_4Ti_3O_{12}$ + $La_4Ti_3O_{12}$ region

The EDS spectrum of area 1 (grey line in Figure 5b) is similar to the spectrum of the previous sample. However, the EDS spectrum of area 2 does not show the peaks of bismuth (black line in Figure 5b). This confirms the results of XRD, which shows the presence of $La_2Ti_2O_7$ (Figure 2b). Figure 4c shows the BEI of the sample $La_{0.48}Bi_{0.023}Li_{0.43}TiO_3$ where two different phases co-exist. The light crystals (area 1 in the picture) correspond to the perovskite-like phase with the same distribution of the elements as in the previous cases (grey line in Figure 5c). The dark ones (area 2) belong to a titanium-rich phase, and the lines of lanthanum and bismuth do not appear in the EDS spectrum (black line in Figure 5c). This agrees with the results of XRD, which show the presence of Li_2TiO_3 (Figure 2c). Finally, Figure 4d shows the BEI of the sample $La_{0.40}Bi_{0.112}Li_{0.47}TiO_3$. We can see three zones. The greyish crystals (area 1 in the picture) belong to a perovskite-like phase with the EDS spectrum shown in Figure 5d (grey line). The dark crystals (area 2 in the picture) correspond to a titanium-rich phase with a similar EDS spectrum

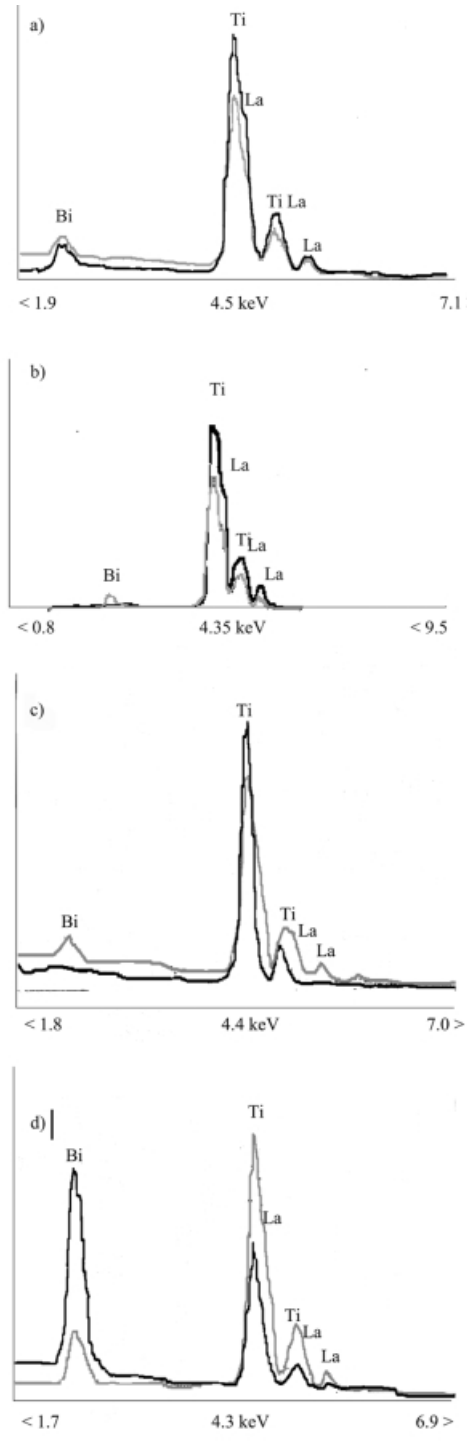

Figure 5. EDS of: a) perovskite-like single-phase solid solution region; b) perovskite-like phase + $La_2Ti_2O_7$ phase; c) perovskite-like phase + Li_2TiO_3 region; d) perovskite-like phase + Li_2TiO_3, + $Bi_4Ti_3O_{12}$ + $La_4Ti_3O_{12}$ region

(black line in Figure 5c and Li_2TiO_3 in the XRD pattern of Figure 2d). The white crystals (area 3 in the picture) are rich in bismuth and titanium but hardly contain lanthanum, as we can see from the EDS spectrum (black line in Figure 5d). This confirms the results of XRD, which showed $Bi_4Ti_3O_{12}$ (Figure 2d). The lanthanum peaks may be due to $La_4Ti_3O_{12}$, as we can see from the XRD pattern (Fig-

ure 2d), or a nearby zone corresponding to the perovskite-like phase.

ICP Analysis

ICP analyses were carried out. We assume that the oxygen content in all the samples is near to 3. For all compositions, the experimental values of Li and Bi were lower than those expected from the starting composition. The results of elemental analyses on mixed regions (Table 1) for different spots matched those for the proposed compounds in Figure 2.

Electrical Measurements (AC)

An HP 4192A Impedance Analyzer was used for AC measurements. These measurements were carried out from 25 °C to 100 °C for compounds on joins $La_{0.46+x}Bi_{0.04}Li_{0.5-3x}TiO_3$ ($0.04 < x < 0.11$) and $La_{0.57-y}Bi_yLi_{0.29}TiO_3$ ($y \leq 0.08$). Two semicircles and a spike were observed in the impedance complex plane plots in all the samples; the second semicircle becomes higher on increasing the amount of bismuth (Figure 6).

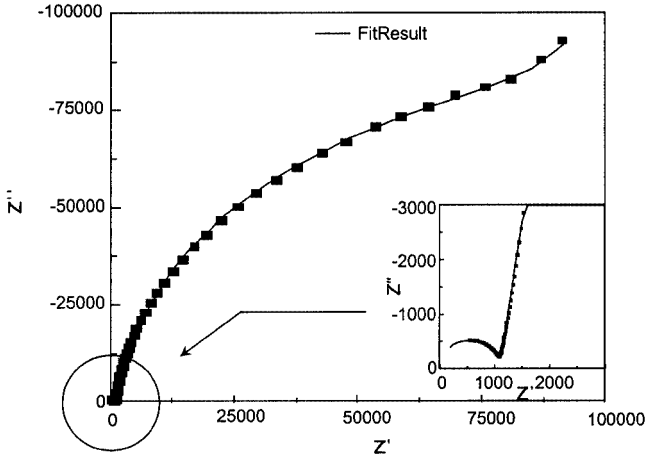

Figure 6. Impedance response at 25 °C for $La_{0.55}Bi_{0.018}Li_{0.29}TiO_3$

The centre of the semicircles was clearly depressed below the baseline, indicating a non-Debye response, which is usual in ionic conductors.[17,18] An equivalent circuit (Figure 7) with two RC and two constant phase elements (CPE)[19] has been used to fit the high frequency data; these elements are assigned to bulk and grain boundary responses with capacities around 20 $pFcm^{-1}$ and 5 $nFcm^{-1}$, respectively. An additional CPE element was used to model the low frequency spike with a capacity around 50 $nFcm^{-1}$.

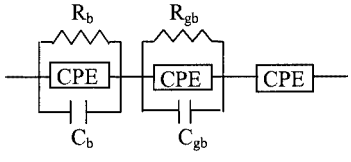

Figure 7. Equivalent circuit for fitting AC data

This value, which is too low for an electrode, has previously been reported for high Na^+ and Li^+ ion conductors,[17,5] and it is attributed to the presence of a Na^+ or Li^+ free layer on the crystal surface. All fitting used the ZView software package.[20]

Bulk conductivity data extracted from the impedance complex plane plots are shown in Arrhenius format for both joins in Figure 8 and Figure 9. Along the join $La_{0.46+x}Bi_{0.04}Li_{0.5-3x}TiO_3$, where the amount of bismuth remains constant, the conductivity is highest when $x = 0.075$, with a conductivity value at 25 °C of 7.59×10^{-4} Scm^{-1}, although the variation in conductivity with composition is quite small (Figure 10). The activation energy increased from 0.310 eV to 0.344 eV. The presence of a maximum in Figure 10 agrees with earlier results for the La system,[2] which report a conduction mechanism based on the A-site vacancies. Along the join $La_{0.57-y}Bi_yLi_{0.29}TiO_3$, where the amount of lithium remains constant, the conductivity decreases when the amount of bismuth increases (Figure 8). However, the substitution of La by Bi is not accompanied by a significant change in the cell volume of the perovskite, so this behaviour does not seem to be related to any change in the "bottleneck" size. However, it could be related to the existence of the lone-electron pair of bismuth.[21,22] Future neutron diffraction studies are underway

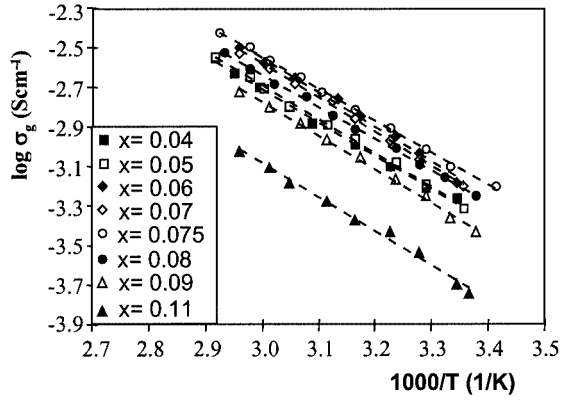

Figure 8. Arrhenius ionic conductivity plots for the join $La_{0.46+x}Bi_{0.04}Li_{0.5-3x}TiO_3$

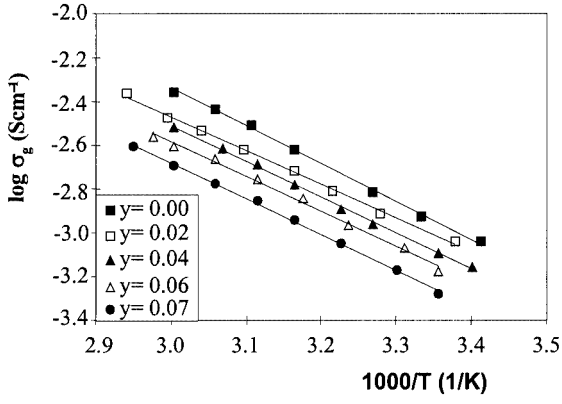

Figure 9. Arrhenius ionic conductivity plots for the join $La_{0.57-y}Bi_yLi_{0.29}TiO_3$

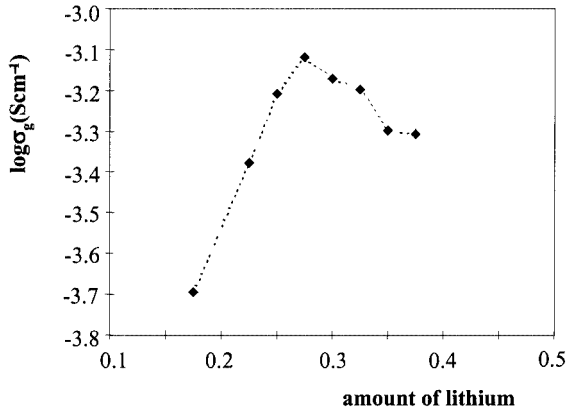

Figure 10. Plot of log σ_b vs. amount of lithium along join $La_{0.46+x}Bi_{0.04}Li_{0.5-3x}TiO_3$

which will give more information about the structure of these compounds and allow us to explain this effect better.

In spite of the good values of bulk conductivity in this system, the samples present significant boundary resistances that are three orders of magnitude higher than the resistances of the bulk, and higher activation energies, around 0.56 eV, which limit the overall conductivity.

Conclusions

Solid solutions with general formula $La_{0.5+x-y}Bi_y$-$Li_{0.5-3x}TiO_3$ have been studied and the results represented on a diagram with corners $La_{2/3}TiO_3$/$La_{0.5}Li_{0.5}TiO_3$/$Bi_{0.5}$-$Li_{0.5}TiO_3$.

Five distinct areas have been found in the diagram. Region A is a melts area, resulting from the melting of the initial mixture. Region B is a mixture of the perovskite-like compound and Li_2TiO_3, $Bi_4Ti_3O_{12}$ and $La_4Ti_3O_{12}$. Region C is a mixture of perovskite-like compounds and $La_2Ti_2O_7$. Region D is a region of perovskite-like solid solutions and region E is a mixture of perovskite-like compound and Li_2TiO_3.

The compounds of general formula $La_{0.5+x-y}Bi_y$-$Li_{0.5-3x}TiO_3$ are ionic conductors. Their ionic conductivity increases when the amount of lithium rises to $x = 0.075$, and the ionic conductivity decreases when the amount of bismuth increases.

Experimental Section

Synthesis: La_2O_3 (99.9% Fluka), TiO_2 (Aldrich 99 +%), Bi_2O_3 (99.9% Aldrich), and Li_2CO_3 (Aldrich >99%) were used as starting materials. La_2O_3 and TiO_2 were dried overnight at 900 °C prior to weighing. These chemicals were weighed, mixed in an agate mortar with acetone, dried, and heated to between 600 and 700 °C for 2 h to drive off CO_2. After grinding, the samples were pressed into pellets and covered with powder of the same composition to avoid loss of lithium and bismuth during the thermal treatment. The pellets were fired at 1100 °C for 12 h giving whitish products which were reground, re-pelleted, and fired at 1200 °C for a further 12 h. Finally, the samples were reground and re-pelleted, fired at 1250 °C for 4 h and quenched to room temperature.

X-ray Diffraction: The solid solution range, crystalline phase identification, and lattice parameters were obtained by powder X-ray diffraction on a Siemens D-500 diffractometer in reflection mode with a detector and a graphite monochromator, using Cu-K_α radiation. Lattice parameters were obtained using a silicon internal standard.

SEM and EDS: Scanning electron microscopy and EDS were obtained with an AN10000 EDS coupled to a JEOL JSM-840 microscope. Stoichiometry was obtained by ICP with a JOVIN IVON instrument.

Electrical Measurements: AC measurements were carried out using an HP 4192A Impedance Analyzer over the range 5 Hz−13 MHz, only in the single phase region. Data correction were carried out in order to avoid the stray capacitance of the jig and the stray inductance and series lead resistance associated with the leads, although data above 5×10^6 Hz were discarded.

Acknowledgments

This work was partially sponsored by financial support from 1999 SGR00044.

[1] M. Itoh, Y. Inaguma, W. Jung, L. Chen, T. Nakamura, *Solid State Ionics* **1994**, *70/71*, 203−207.
[2] H. Kawai, J. Kuwano, *J. Electrochem. Soc.* **1994**, *141*, L78−L79.
[3] Y. Inaguma, L. Chen, M. Itoh, T. Nakamura, *Solid State Ionics* **1994**, *70/71*, 196−202.
[4] A. D. Robertson, S. García Martín, A. Coats, A. R. West, *J. Mater. Chem.* **1995**, *5*, 1405−1412.
[5] M. Morales, A. R. West, *Solid State Ionics* **1996**, *91*, 33−43.
[6] J. M. S. Skakle, G. C. Mather, M. Morales, R. I: Smith, A. R. West, *J. Mater. Chem.* **1995**, *5*, 1807−1808.
[7] R. I. Smith, J. M. S. Skakle, G. C. Mather, M. Morales, A. R. West, *Mater. Sci. Forum* **1996**, *228−231*, 701−704.
[8] M. Morales, M. L. Martízez−Sarrión, *J. Mater. Chem.* **1998**, *8*, 1583−1587.
[9] I. Moreno, M. Morales, M. L. Martínez−Sarrión, *J. Solid State Chem.* **1998**, *140*, 377−386.
[10] M. L. Martínez−Sarrión, L. Mestres, M. Morales, M. Herráiz, *J. Solid State Chem.* **2000**, *154*, 280−285.
[11] E. M. Levin, R. S. Roth, *J. Res. Nat. Bur. Stand.* **1964**, *68A*, 197.
[12] F. Abraham, M. F. Debreuille−Gresse, G. Mairesse, G. Nowogrocki, *Solid State Ionics* **1988**, *28−30*, 529−532.
[13] C. K. Lee, D. C. Sinclair, A. R. West, *Solid State Ionics* **1993**, *62*, 193−198.
[14] C. K. Lee, G. S. Lim, A. R. West, *J. Mater. Chem.* **1994**, *4*, 1441−1444.
[15] Y. Inaguma, M. Itoh, *Solid State Ionics* **1996**, *86−88*, 257−260.
[16] J. L. Fourquet, H. Duroy, M. P. Crosnier-Lopez, *J. Solid State Chem.* **1996**, *127*, 283−294.
[17] A. K. Jonscher, J. M. Reau, *J. Mater. Sci.* **1978**, *13*, 563−570.
[18] P. G. Bruce, A. R. West, D. P. Almond, *Solid State Ionics* **1982**, *7*, 57−60
[19] A. K. Jonscher, in "Dielectric Relaxation in Solids", Chap. 5. Chelsea Dielectric, London (1983)
[20] ZView for windows (ver. 1.4), Scribner Assoc. Inc., Charlatesville, Virginia, USA.
[21] P. Lacorre, *Solid State Sciences* **2000**, *2*, 755−758.
[22] F. Goutenoire, O. Isnard, E. Suard, O. Bohnke, Y. Laligant, R. Retoux, P. Lacorre, *J. Mater. Chem.* **2001**, *11*, 119−124.

Received October 30, 2001
[I01428]